Local metal-insulator transition in a generalised impurity Anderson model

Abhirup Mukherjee[1,*] and Siddhartha Lal[1,†]

[1] *Department of Physical Sciences, Indian Institute of Science Education and Research-Kolkata, W.B. 741246, India*

(Dated: April 29, 2022)

Lorem ipsum dolor sit amet, consectetur adipiscing elit, sed do eiusmod tempor incididunt ut labore et dolore magna aliqua. Ut enim ad minim veniam, quis nostrud exercitation ullamco laboris nisi ut aliquip ex ea commodo consequat. Duis aute irure dolor in reprehenderit in voluptate velit esse cillum dolore eu fugiat nulla pariatur. Excepteur sint occaecat cupidatat non proident, sunt in culpa qui officia deserunt mollit anim id est laborumLorem ipsum dolor sit amet, consectetur adipiscing elit, sed do eiusmod tempor incididunt ut labore et dolore magna aliqua. Ut enim ad minim veniam, quis nostrud exercitation ullamco laboris nisi ut aliquip ex ea commodo consequat. Duis aute irure dolor in reprehenderit in voluptate velit esse cillum dolore eu fugiat nulla pariatur. Excepteur sint occaecat cupidatat non proident, sunt in culpa qui officia deserunt mollit anim id est laborumLorem ipsum dolor sit amet, consectetur adipiscing elit, sed do eiusmod tempor incididunt ut labore et dolore magna aliqua. Ut enim ad minim veniam, quis nostrud exercitation ullamco laboris nisi ut aliquip ex ea commodo consequat. Duis aute irure dolor in reprehenderit in voluptate velit esse cillum dolore eu fugiat nulla pariatur. Excepteur sint occaecat cupidatat non proident, sunt in culpa qui officia deserunt mollit anim id est laborum

I. INTRODUCTION

The Hubbard model is one of the fundamental models for strong electronic correlation; in its simplest form, it features a single band of conduction electrons hopping on a lattice and interacting via local correlations that provide a cost U if any site is doubly occupied:

$$H_{\text{hubb}} = -t \sum_{\langle i,j\rangle,\sigma} \left(c^\dagger_{i\sigma} c_{j\sigma} + \text{h.c.} \right) + U \sum_i \hat{n}_{i\uparrow}\hat{n}_{i\downarrow} - \mu \sum_{i,\sigma} \hat{n}_{i\sigma}$$

The model can be made particle-hole symmetric by choosing $\mu = U/2$:

$$H_{\text{hubb}} = -t \sum_{\langle i,j\rangle,\sigma} \left(c^\dagger_{i\sigma} c_{j\sigma} + \text{h.c.} \right) - \frac{U}{2} \sum_i (\hat{n}_{i\uparrow} - \hat{n}_{i\downarrow})^2$$

There are two trivial limits of the model. At $U = 0$, the bath consists of just a kinetic energy part, and the ground state is just a filled Fermi sea. At $t = 0$, each lattice site decouples from the rest and becomes a local moment, which under symmetry-breaking becomes a Neel antiferromagnet. This suggests that on increasing U/t beyond some critical value, the system might undergo a phase transition from a metallic state to an insulating state [1]. This transition is reflected in the local spectral function - while it has a well-defined zero energy peak in the metallic phase, it is gapped in the insulating phase.

One method of studying Hubbard models is through auxiliary models, described in the next section. Auxiliary models are simpler versions of the full Hamiltonian that are able to capture the essential physics. For eg, a correlated impurity interacting with a conduction bath is a potential auxiliary model for the Hubbard Hamiltonian: The impurity has onsite energy ϵ_d and an onsite correlation U. It hybridises into the bath through V.

If the impurity site hybridises with a *non-interacting* bath defined by a uniform density of states, the impurity spectral function is found to have a well-defined Kondo resonance at low temperatures. Increasing the impurity correlation U only serves to reduce the width of the central peak at the cost of the appearance of side bands at energy scales of the order of U, but the resonance never dies. The situation is however different if the impurity is embedded in a correlated conduction bath with a non-trivial density of states. For the case of a conduction band with the DOS shown in the right of the figure below, the impurity hybridises into a reduced bandwidth because of the correlation on the lattice [2].

This difference in the type of conduction baths is utilized in dynamical mean-field theory to describe various phases of the bulk system. This is done through the DMFT algorithm: one starts with a non-interacting bath, but depending on the value of U, the conduction bath then gets modified and we ultimately end up with something that is different from what we started with. For small U, the bath does not change much and we retain the central resonance of the impurity spectral function. This then describes a metal in the bulk. For larger values of U, however, the bath changes significantly such that its density of states becomes non-constant. Above a critical U_c, the impurity spectral function gets gapped out, and that then describes the insulating phase in the bulk. *This leaves open the following question*: What is the minimal correlation one can insert into the non-interacting bath (of a single-impurity Anderson model) that can capture both the metallic and insulating phases of the bulk model?

Lorem ipsum dolor sit amet, consectetur adipiscing elit, sed do eiusmod tempor incididunt ut labore et dolore magna aliqua. Ut enim ad minim veniam, quis nos-

* am18ip014@iiserkol.ac.in
† slal@iiserkol.ac.in

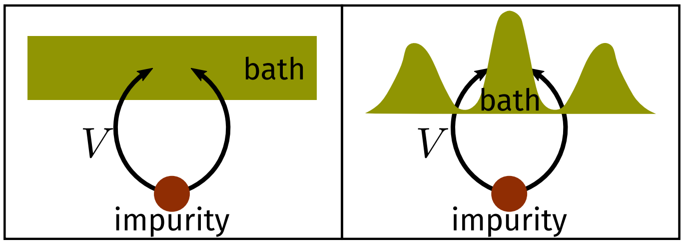

FIG. 1. Two kinds of bath that an impurity can hybridise into. The left panel shows a non-interacting conduction band with a flat density of states. The right panel shows an interacting bath with an energy-dependent density of states. In the latter case, the impurity "feels" a reduced effective bandwidth defined by the width of the central peak.

trud exercitation ullamco laboris nisi ut aliquip ex ea commodo consequat. Duis aute irure dolor in reprehenderit in voluptate velit esse cillum dolore eu fugiat nulla pariatur. Excepteur sint occaecat cupidatat non proident, sunt in culpa qui officia deserunt mollit anim id est laborum Lorem ipsum dolor sit amet, consectetur adipiscing elit, sed do eiusmod tempor incididunt ut labore et dolore magna aliqua. Ut enim ad minim veniam, quis nostrud exercitation ullamco laboris nisi ut aliquip ex ea commodo consequat. Duis aute irure dolor in reprehenderit in voluptate velit esse cillum dolore eu fugiat nulla pariatur. Excepteur sint occaecat cupidatat non proident, sunt in culpa qui officia deserunt mollit anim id est laborum Lorem ipsum dolor sit amet, consectetur adipiscing elit, sed do eiusmod tempor incididunt ut labore et dolore magna aliqua. Ut enim ad minim veniam, quis nostrud exercitation ullamco laboris nisi ut aliquip ex ea commodo consequat. Duis aute irure dolor in reprehenderit in voluptate velit esse cillum dolore eu fugiat nulla pariatur. Excepteur sint occaecat cupidatat non proident, sunt in culpa qui officia deserunt mollit anim id est laborum Lorem ipsum dolor sit amet, consectetur adipiscing elit, sed do eiusmod tempor incididunt ut labore et dolore magna aliqua. Ut enim ad minim veniam, quis nostrud exercitation ullamco laboris nisi ut aliquip ex ea commodo consequat. Duis aute irure dolor in reprehenderit in voluptate velit esse cillum dolore eu fugiat nulla pariatur. Excepteur sint occaecat cupidatat non proident, sunt in culpa qui officia deserunt mollit anim id est laborum Lorem ipsum dolor sit amet, consectetur adipiscing elit, sed do eiusmod tempor incididunt ut labore et dolore magna aliqua. Ut enim ad minim veniam, quis nostrud exercitation ullamco laboris nisi ut aliquip ex ea commodo consequat. Duis aute irure dolor in reprehenderit in voluptate velit esse cillum dolore eu fugiat nulla pariatur. Excepteur sint occaecat cupidatat non proident, sunt in culpa qui officia deserunt mollit anim id est laborumLorem ipsum dolor sit amet, consectetur adipiscing elit, sed do eiusmod tempor incididunt ut labore et dolore magna aliqua. Ut enim ad minim veniam, quis nostrud exercitation ullamco laboris nisi ut aliquip ex ea commodo consequat. Duis aute irure dolor in reprehenderit in voluptate velit esse cillum dolore eu fugiat nulla pariatur. Excepteur sint occaecat cupidatat non proident, sunt in culpa qui officia deserunt mollit anim id est laborumLorem ipsum dolor sit amet, consectetur adipiscing elit, sed do eiusmod tempor incididunt ut labore et dolore magna aliqua. Ut enim ad minim veniam, quis nostrud exercitation ullamco laboris nisi ut aliquip ex ea commodo consequat. Duis aute irure dolor in reprehenderit in voluptate velit esse cillum dolore eu fugiat nulla pariatur. Excepteur sint occaecat cupidatat non proident, sunt in culpa qui officia deserunt mollit anim id est laborum

II. THE GENERALISED ANDERSON IMPURITY MODEL

The impurity models we will work with couple the impurity to a single site in the lattice. We will refer to that specific site as the zeroth site throughout. We recall the Hamiltonian of the Anderson impurity model with a half-filled impurity site:

$$\mathcal{H} = \frac{-U}{2}\left(\hat{n}_{d\uparrow} - \hat{n}_{d\downarrow}\right)^2 + \sum_{\vec{k},\sigma} \epsilon_{\vec{k}} \tau_{\vec{k},\sigma} + V \sum_{\sigma} \left(c^{\dagger}_{d\sigma} c_{0\sigma} + \text{h.c.} \right) , \tag{1}$$

where $\tau_{\vec{k},\sigma} \equiv \hat{n}_{\vec{k},\sigma} - 1/2$. Also, $c_{d\sigma}$ and $c_{0\sigma}$ are the fermionic annihilation operators of spin σ for the impurity and zeroth sites respectively. U is the repulsive correlation on the impurity site, and the impurity is at particle-hole symmetry. V is the momentum-independent hybridisation parameter that couples the impurity with the lattice. We will work with a constant density of states in the bath.

In order to enhance the Anderson impurity model, we introduce two extra two-particle interaction terms into the Hamiltonian:

- a spin-exchange term $J\vec{S}_d \cdot \vec{s}_0$ between the impurity spin $\vec{S}_d$ and the spin $\vec{s}_0$ of the zeroth site
- a local correlation term $U_b \hat{n}_{0\uparrow}\hat{n}_{0\downarrow}$ on the zeroth site

With these additional terms, the *generalised Anderson impurity model* (hence referred to as the GAIM), at particle-hole symmetry, is

$$\mathcal{H} = \frac{-U}{2}\left(\hat{n}_{d\uparrow} - \hat{n}_{d\downarrow}\right)^2 + \sum_{\vec{k},\sigma} \epsilon_{\vec{k}} \tau_{\vec{k},\sigma} + V \sum_{\sigma} \left(c^{\dagger}_{d\sigma} c_{0\sigma} + \text{h.c.} \right) + J\vec{S}_d \cdot \vec{s}_0 + U_b \hat{n}_{0\uparrow}\hat{n}_{0\downarrow} \tag{2}$$

All the terms in the Hamiltonian have been depicted schematically in fig. 2.

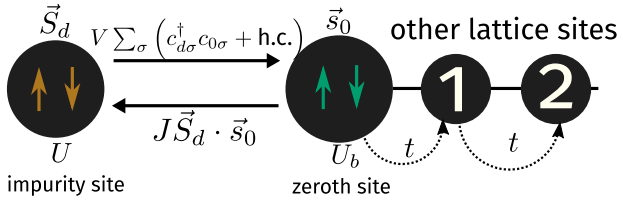

FIG. 2. While we have studied the full model under renormalisation group, often we will turn to a simplified zero-bandwidth version of the model that is obtained by ignoring the kinetic energy part of the Hamiltonian. This zero-bandwidth model is effectively a two site model.

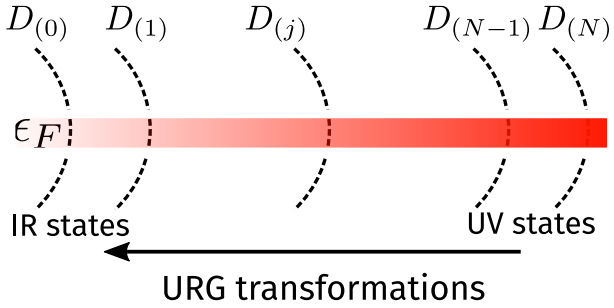

FIG. 3. High energy - low energy scheme defined and used in the URG method. The states away from the Fermi surface form the UV subspace and are decoupled first, leading to a Hamiltonian which is more block-diagonal and comprised of only the IR states near the Fermi surface.

III. METHOD AND RG EQUATIONS

A. The unitary RG method

The focus here is on obtaining the low-energy phases of the GAIM. To accomplish this, we perform a renormalisation group analysis of the associated Hamiltonian (eq. 2) using the recently developed unitary renormalisation group (URG) method [3–11]. The unitary RG transformations lead to a series of Hamiltonians $H_{(j)}$ related to the Hamiltonian at the previous step through a unitary transformation; the unitary transformations are defined by the requirement that they remove number fluctuations in high-energy $k-$states, thus making the Hamiltonian progressively more block-diagonal in momentum space. The high-energy degrees of freedom that get decoupled in the process become integrals of motion (IOMs) for the Hamiltonian and enter the Hamiltonian only in a purely number-diagonal form.

To be more precise, we first choose a complete basis $\{|j\rangle\}$ and arrange these states from high-energy (UV) to low-energy (IR). Typically we take these states to be the momentum eigenstates $\left(|j\rangle = \left\{|\vec{k}\uparrow\rangle, |\vec{k}\downarrow\rangle\right\}\right)$, and the isoenergetic shells $\left\{D_{(j)}\right\}$ then define the sequence of states, such that the momenta far away from the Fermi surface (taken to be at higher j and having $|D_{(j)}| \gg |\epsilon_F|$) are taken to be the UV states while those near the Fermi surface (taken to be at lower j and having $D_{(j)} \sim \epsilon_F$) comprise the IR states. This scheme is shown in fig. 3.

At a given RG step j, the Hamiltonian $H_{(j)}$ involves number fluctuations between the $k-$states that have energies lower than $D_{(j+1)}$. So the most energetic states that are still non-trivially present in $H_{(j)}$ are those on the energy contour $D_{(j)}$, and the Hamiltonian $H_{(j)}$ will, in general, not conserve the number of particles in this energy (or momentum) state: $\left[H_{(j)}, \hat{n}_j\right] \neq 0$. The unitary transformation $U_{(j)}$ is then defined so as to remove this number fluctuation at the next RG step [5, 6]:

$$H_{(j-1)} = U_{(j)} H_{(j)} U^\dagger_{(j)} \ , \ \left[H_{(j-1)}, \hat{n}_j\right] = 0 \ . \tag{3}$$

The unitary transformations can be expressed in terms of a generator $\eta_{(j)}$ that has fermionic algebra [5, 6]:

$$U_{(j)} = \frac{1}{\sqrt{2}}\left(1 + \eta_{(j)} - \eta^\dagger_{(j)}\right) \ , \quad \left\{\eta_{(j)}, \eta^\dagger_{(j)}\right\}_\pm = 1 \ , \tag{4}$$

where $\{A, B\}_\pm = AB \pm BA$. The generator itself is given by the expression [5, 6]

$$\eta^\dagger_{(j)} = \frac{1}{\hat{\omega}_{(j)} - \text{Tr}\left(H_{(j)}\hat{n}_j\right)} c^\dagger_j \text{Tr}\left(H_{(j)} c_j\right) \ . \tag{5}$$

The important operator $\hat{\omega}_{(j)}$ originates from the quantum fluctuations that exist in the problem because of the non-commutation of the kinetic energy terms and the interaction terms in the Hamiltonian:

$$\hat{\omega}_{(j)} = H_{(j-1)} - H^i_{(j)} \ . \tag{6}$$

$H^i_{(j)}$ is the part of $H_{(j)}$ that commutes with $\hat{n}_j$ but does *not* commute with at least one $\hat{n}_l$ for $l < j$. The RG flow continues up to energy D^*, where a fixed point is reached from the vanishing of the RG function.

B. URG equations for the GAIM

The derivation of the RG equations for the generalised Anderson impurity model Hamiltonian is shown in the appendix. We provide below the RG equations for a given quantum fluctuation scale ω:

$$\Delta U_b = 0 \ , \tag{7}$$

$$\Delta U = 4V^2 n_j \left(\frac{1}{d_1} - \frac{1}{d_0}\right) - n_j \frac{J^2}{d_2} \ , \tag{8}$$

$$\Delta V = -\frac{3n_j V}{8}\left[J\left(\frac{1}{d_2} + \frac{1}{d_1}\right) + \frac{4U_b}{3}\sum_{i=1}^{4}\frac{1}{d_i}\right] \ , \tag{9}$$

$$\Delta J = -\frac{n_j J\left(J + 4U_b\right)}{d_2} \ . \tag{10}$$

The denominators d_i used in these equations are given by

$$d_0 = \omega - \frac{D}{2} + \frac{U_b}{2} - \frac{U}{2} \ , \tag{11}$$

$$d_1 = \omega - \frac{D}{2} + \frac{U_b}{2} + \frac{U}{2} + \frac{J}{4} \ , \tag{12}$$

$$d_2 = \omega - \frac{D}{2} + \frac{U_b}{2} + \frac{J}{4} \ , \tag{13}$$

$$d_3 = \omega - \frac{D}{2} + \frac{U_b}{2} \ . \tag{14}$$

The symbols used in the RG equations have the following meanings: ΔU represents the renormalisation in the coupling U in going from the j^{th} Hamiltonian to the $(j-1)^{\text{th}}$ Hamiltonian by decoupling the isoenergetic shell at energy $D_{(j)}$. n_j is the number of electronic states on the shell $D_{(j)}$.

We will discuss the consequences of these RG equations in the next sections, but we clarify here that the labels U_0, J_0, V_0 that might occur in the figures or elsewhere in the text represent the bare values of the associated couplings U, J and V. We also point out here that throughout the upcoming results, the bare value of U_b is set to the negative of the bare value of U_0: $U_b = -U_0/10$. This means that whenever we vary U_0 along the axis of a plot, we are simultaneous varying U_b. The reason for choosing the negative sign of U_b will be clarified in the next section.

IV. RG FLOWS AND PHASE DIAGRAM

We start the discussion on the nature of the RG flows by noting that the bath correlation U_b is marginal, and the spin-exchange coupling J has a critical point ($\Delta J = 0$) at $U_b = -J/4$. We will look at the RG flows of the couplings U, V and J on both sides of this critical point, and see what phases they lead to. We will work in the regime of quantum fluctuations where all the denominators are negative: $d_i < 0 \ \forall \ i$. Before we start, note that:

- Since J is positive, this means that we can capture both relevant and irrelevant RG flows of J by keeping U_b negative. U_b is found to be marginal under the RG transformation, and we set U_b to $-U_0/10$ hereafter.
- The critical point has been chosen from the RG equation of J and not of V; this is because, the RG irrelevance of J is sufficient to make V irrelevant as well, and on the other hand, the RG relevance of J is sufficient to screen the impurity.

A. RG flows for $4U_b + J_0 > 0$

In this regime, J is relevant and flows to large positive values. It is also easy to deduce from its RG equation that V is also relevant. U is more non-trivial, because its RG equation involves both V and J. Nevertheless, the RG equations were solved numerically with bare values of the couplings and the bandwidth, and it was found that while V and J are relevant, U is irrelevant. These findings are shown in the blue curves of fig. 4. The fixed point values can be summarised as:

$$U^* = 0, \quad V^* \gg 1, \quad J^* \gg 1, \quad U_b \sim \mathcal{O}(1) \tag{15}$$

B. RG flows for $4U_b + J_0 < 0$

The RG β-function function for J changes sign as we tune U_b to less than $-J_0/4$, and J becomes irrelevant. As for V, note that in the RG equation for V, it is J that drives V to be relevant while U_b drives V to irrelevance; if J itself is irrelevant, then ΔV will be dominated by U_b and V will be ultimately irrelevant. The behaviour of U is again non-trivial and ananlytically not tractable, so we solve the RG equations numerically. It turns out that although U is slightly irrelevant, it saturates to an appreciable value near the fixed point. These RG flows are shown in the purple curves of fig. 4. The fixed point values in this regime can be summarised as:

$$U^* \sim \mathcal{O}(1), \quad V^* = 0, \quad J^* = 0, \quad U_b \sim \mathcal{O}(1) \tag{16}$$

C. Phase diagram: impurity phase transition

The low-energy RG phase diagram is obtained by solving the RG equations for ranges of couplings, and is shown in fig. 5. There are four distinct phases in the space of couplings U_0 vs J_0, with U_b constrained at $-U_0/10$ and V_0 set to $2J_0$. The purple phase (phase B in the legend) is composed of those Hamiltonians which lead to RG relevant V, J and RG irrelevant U. In other words, this is the phase where the impurity moment is screened by the conduction electrons. This is the low-energy phase of the usual Anderson impurity model that has U and V. The red phase (phase C in the legend) consists of those Hamiltonians which produce irrelevant J, V and a relevant U; here, the conduction electrons fail to screen the impurity and a residual local moment survives on the impurity at low energies. The light green phase (phase D in the legend) lies in between these two phases, and is defined by non-negligible V^*, U^* but zero J^*. In this phase, the impurity still gets screened, but there is more charge content on the impurity site compared to phase B. On going to the thermodynamic limit by increasing the bandwidth D_0, this light green phase disappears. The gray phase (phase A in the legend) is a "dead" phase where U, V, J are all RG irrelevant. The various phases are summarised in table. I.

The black line in fig. 5 represents a line of critical points $U_b = J_0$, and separates the two major phases of the impurity. Such a *phase transition* between the screened

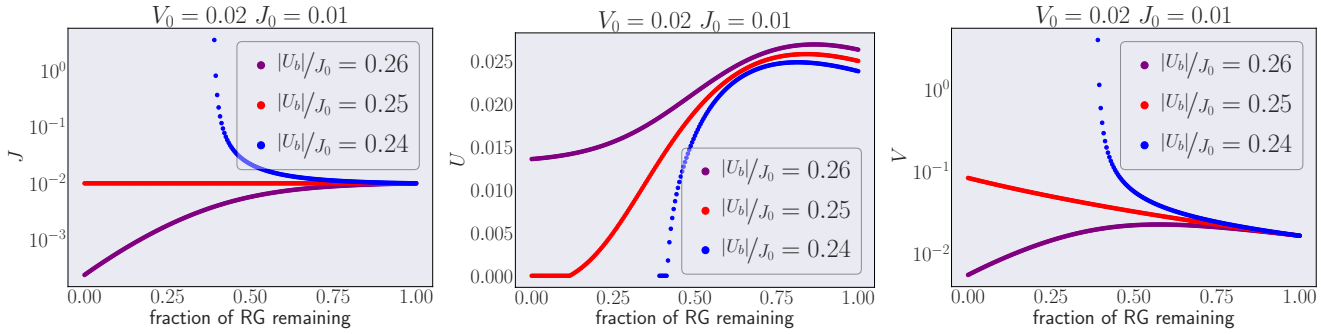

FIG. 4. Variation of couplings U, V and J along the RG transformations. x-axis represents the RG steps, the rightmost point is the first RG step and leftmost point is the final RG step. The values of the bare couplings are given in the title. All values are in units of the half-bandwidth D_0, which is chosen to be 10. The blue curves represent the flows for $4U_b + J > 0$, where J is relevant. The purple curves represent the RG flows for $4U_b + J < 0$, where J is irrelevant. The red curves are exactly at the critical point, where J is marginal.

impurity and the local moment phases is absent in the usual Anderson impurity model without the attractive correlation U_b. In fact, only the purply screened phase is adiabatically connected the Anderson impurity model.

phase	RG flow	fixed point
B	$\Delta U < 0, \Delta J, \Delta V > 0$	$U^* \ll V^* \ll J^*$
D	$\Delta U, \Delta J < 0, \Delta V > 0$	$J^* < U^* \ll V^*$
C	$\Delta U > 0, \Delta J, \Delta V < 0$	$U^* \gg 1, V^*, J^* = 0$
A	$\Delta U, \Delta J, \Delta V < 0$	$U^*, V^*, J^* = 0$

TABLE I. Summary of the various fixed point phases

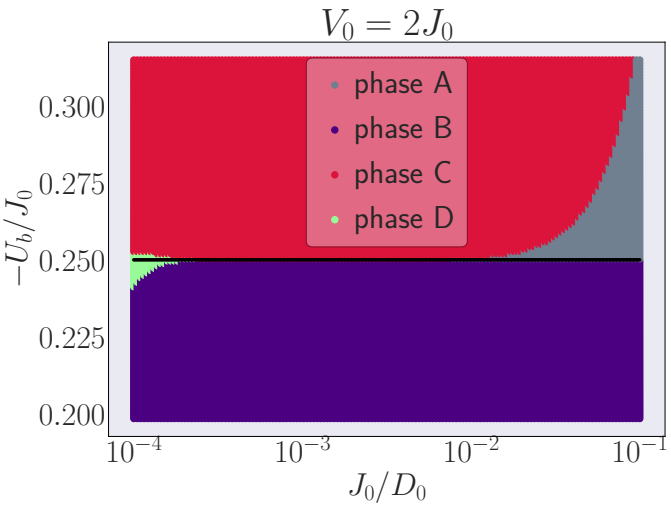

FIG. 5. Phase diagram of the GAIM, in the space of couplings U_0 and J_0. U_b is set to $-U_0/10$ and V_0 is set to $2J_0$. The various phases A through D are characterised in the text.

V. LOW-ENERGY EFFECTIVE HAMILTONIAN AND THE GROUND STATE

The RG fixed point Hamiltonian describes the low-energy phase of the system. In general, if the RG fixed point is reached at an energy scale D^*, the fixed point Hamiltonian $\mathcal{H}^*$ is obtained simply from the fixed point values of the couplings, and by noting that the states above D^* are now part of the IOMs:

$$\mathcal{H}^* = \frac{-U^*}{2}\left(\hat{n}_{d\uparrow} - \hat{n}_{d\downarrow}\right)^2 + \sum_{\sigma,\vec{k}:|\epsilon_{\vec{k}}|<D^*} \epsilon_{\vec{k}} \tau_{\vec{k},\sigma} + U_b^* \hat{n}_{0\uparrow}\hat{n}_{0\downarrow} + V^* \sum_{\sigma} \left(c_{d\sigma}^\dagger c_{0\sigma} + \text{h.c.}\right) + J^* \vec{S}_d \cdot \vec{s}_0 \tag{17}$$

A. Screened regime: $-U_b/J < 1/4$

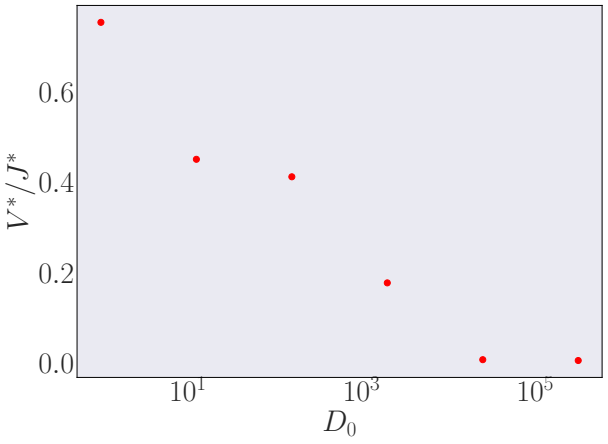

The fixed point Hamiltonian can, in general, be written

as

$$\mathcal{H}^* = \sum_{\sigma,k} \epsilon_k \tau_{k\sigma} - \frac{U^*}{2}\left(\hat{n}_{d\uparrow} - \hat{n}_{d\downarrow}\right)^2 + \sum_{\sigma,k<\Lambda^*}\left(V^* c^\dagger_{k\sigma} c_{d\sigma} + \text{h.c.}\right) + J^* \vec{s}\cdot\vec{S} \tag{18}$$

The first term is the kinetic energy of all the electrons. The next two terms are the impurity-diagonal pieces, featuring the renormalised interaction U^*. The next three terms are the residual interactions between the impurity and the metal, with the renormalised couplings V^*, J^* and K^*. The summations in these terms extend from the fixed point momentum cutoff Λ^* to 0. This is the region of momentum space which the URG was unable to decouple. The operators $\vec{s}$ and $\vec{C}$ represent the macroscopic magnetic and charge spins formed by the remaining electrons that are lying inside the window $[0, \Lambda^*]$:

$$\vec{s} = \sum_{\substack{kk'<\Lambda^* \\ \alpha\beta}} c^\dagger_{k\alpha} \vec{\sigma}_{\alpha\beta} c_{k'\beta} \tag{19}$$

Our goal here is to write down the ground state wavefunction for this low-energy Hamiltonian.

To make progress, we will simplify the effective Hamiltonian by taking the zero bandwidth limit. This reduces it to a two-site problem. One site is of course the impurity site, and this site will be labeled as site 1. The other site will be formed by the center of mass degree of freedom of the conduction electrons, and will be labeled as site 2. The Hamiltonian for this two-site problem is

$$\mathcal{H}_{IR} = -\frac{U^*}{2}\left(\hat{n}_{1\uparrow} - \hat{n}_{1\downarrow}\right)^2 + V^* \sum_\sigma \left(c^\dagger_{1\sigma} c_{2\sigma} + \text{h.c.}\right) + J^* \vec{S}_1 \cdot \vec{S}_2 + K^* \vec{C}_1 \cdot \vec{C}_2 \tag{20}$$

The subscripts on the operators designate the site on which they act; $\hat{n}_1$ is the number operator for the first site.

We will adopt the following notation to represent the states in this Hilbert space. A general state will be represented in the Fock space basis as $|n_{1\uparrow} n_{1\downarrow} n_{2\uparrow} n_{2\downarrow}\rangle$. For example,

$$|1101\rangle = c^\dagger_{1\uparrow} c^\dagger_{1\downarrow} c^\dagger_{2\downarrow} |-\rangle \tag{21}$$

$|-\rangle$ is the vacuum state.

For $U > 0$, the ground state is given by

$$|\Psi\rangle_1 = c_s \frac{1}{\sqrt{2}}\left(|\uparrow,\downarrow\rangle - |\downarrow,\uparrow\rangle\right) + c_c \frac{1}{\sqrt{2}}\left(|\uparrow\downarrow,0\rangle + |0,\uparrow\downarrow\rangle\right), \quad E_1 = -V^* \sqrt{\gamma^2+4} - \frac{1}{4}U^* - \frac{3}{8}J^* \tag{22}$$

where $\gamma = \frac{1}{2V^*}\left[\frac{1}{4}\left(3J^* + K^*\right) + \frac{1}{2}U^*\right]$. The probabilities for the spin and charge sectors for the ground state are

$$\begin{aligned} \left(c_s\right)^2 &= \frac{1}{2\sqrt{\gamma^2+4}}\left(\sqrt{\gamma^2+4} + \gamma\right), \\ \left(c_c\right)^2 &= \frac{1}{2\sqrt{\gamma^2+4}}\left(\sqrt{\gamma^2+4} - \gamma\right). \end{aligned} \tag{23}$$

For (roughly) $J_0 > V_0$, we get $J^* \gg V^*$ and $U^* \gg U_0$ so that $\gamma \gg 1$. This gives $\left(c_s\right)^2 \sim 1$ and $\left(c_c\right)^2 \sim 0$. The entire contribution to the ground state then comes from the spin sectors of the two sites. This is calculated numerically in fig. 6.

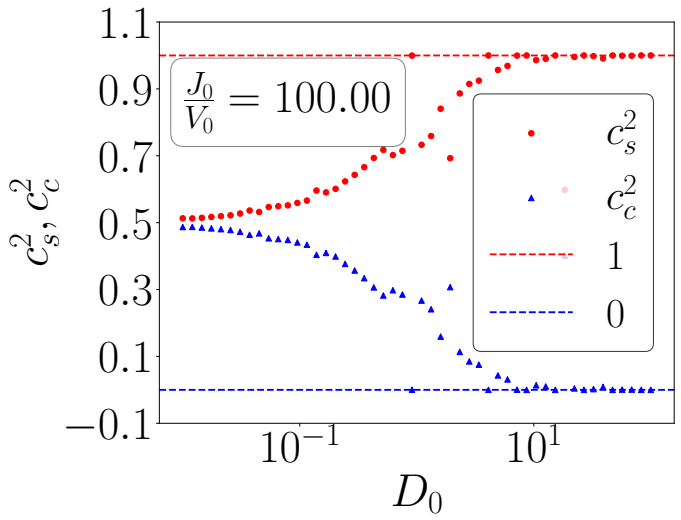

FIG. 6. Variation of relative weights c_s and c_c with J_0

In the other regime of $U < 0$, the two competing states are $|\Psi\rangle_1$ defined above (with energy E_1), and $|\Psi_2\rangle$, the charge singlet: $|\Psi\rangle_2 = \frac{1}{\sqrt{2}}\left(|2,0\rangle - |0,2\rangle\right)$ having energy E_2.

$$E_2 = -\frac{3}{4}K^*, \quad E_1 - E_2 = -\frac{1}{4}\sqrt{\left(\frac{1}{2}K^* + U^*\right)^2 + (4V^*)^2} - \frac{1}{4}U^* + \tag{24}$$

For $V_0 \gg K_0$, the largest energy scale will be V^*, and we can then approximate this difference as

$$E_1 - E_2 \simeq -V^* < 0 \tag{25}$$

In such a case, $|\Psi\rangle_1$ will therefore be the ground state. In the other regime $V_0 \ll K_0$, the largest energy scale will be K^*, and we can then write

$$E_1 - E_2 \simeq -\frac{1}{8}K^* + \frac{3}{4}K^* > 0 \tag{26}$$

In this case, the ground state will be $|\Psi\rangle_2$. There exists, therefore, a phase transition at a critical plane (U_c, K_c, V_c), where the ground state changes between the charge singlet $|\Psi\rangle_2$ and the spin singlet + charge triplet $|\Psi\rangle_1$.

B. Unscreened regime: $-U_b/J > 1/4$

C. Approach towards the thermodynamic limit

[Update with V vs D plots]

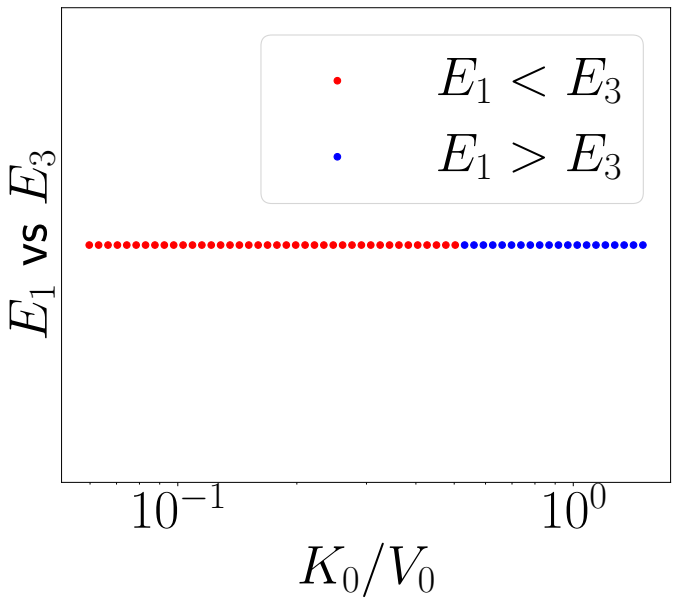

The URG method works strictly on finite systems and leads to finite values of fixed point couplings. The behaviour of the Hamiltonian in the thermodynamic limit can then be determined using finite-size scaling where we increase the bandwidth and decrease the width of each RG step. When applied to the fixed point value of the impurity-bath hybridisation parameter V (fig. 7), it can be seen that the fixed point value increases as the system size is increased, implying that the continuum limit of V^* is ∞. This holds for both $V_0 > J_0$ and $V_0 < J_0$, as shown in the two panels of fig. 7.

In a similar manner, we checked the variation of the spin and charge probabilities, c_s and c_c, in the ground state, with increasing bandwith. The result is shown in fig. 8. For both $V_0 < J_0$ and $V_0 > J_0$, we see that the spin contribution increases towards unity while the charge contribution vanishes. This indicates that at large bandwidth, the ground state becomes purely a spin singlet, formed purely by singly-occupied impurity states.

$$\lim_{D_0 \to \infty} |\Psi\rangle_1 = \frac{1}{\sqrt{2}} \left(|\uparrow, \downarrow\rangle - |\downarrow, \uparrow\rangle \right) \tag{27}$$

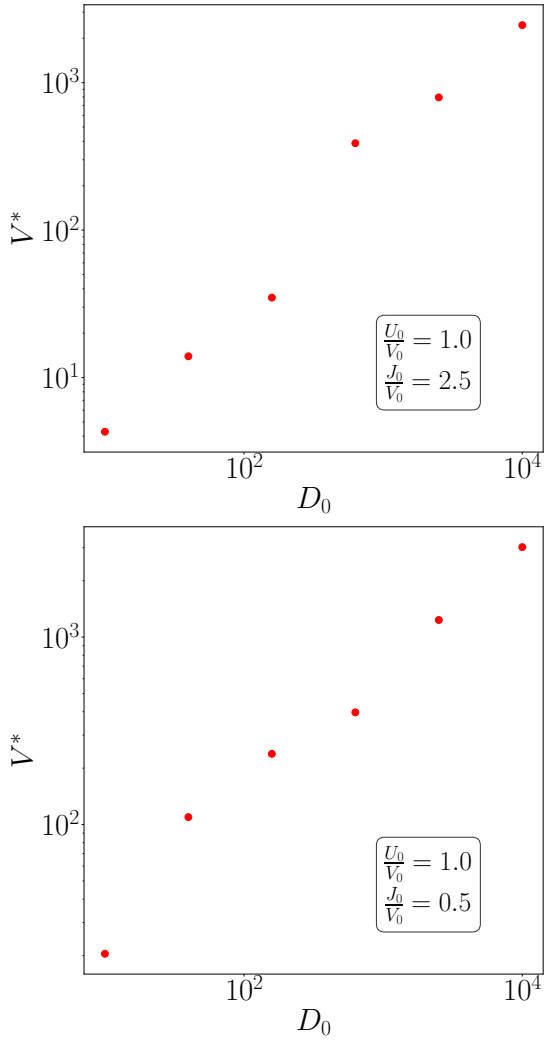

FIG. 7. Variation of fixed point value V^* with increasing bandwith D_0, for both $V_0 > J_0$ and $V_0 < J_0$.

D. The critical point: $-U_b/J = 1/4$

VI. EVOLUTION OF THE GROUNDSTATE ACROSS THE TRANSITION

Overlap of ground state against spin singlet and charge triplet zero states

A. Presence of sub-dominant pair fluctuations

The behaviour of the various kinds of correlation functions (for eg., the reduction of the impurity compensation $\vec{S}_d \cdot \vec{s}_0$) shown above indicate that the Kondo cloud that screens the impurity is getting destroyed as U_b/J increases in magnitude. To shed some light on the nature of the fluctuations that faciliate this process, we also plot the average pair fluctuation in the ground state as a function of U_b/J, in fig. 9. The pair fluctuations are terms that transfer an electron pair between the impurity and zeroth sites: $c^\dagger_{d\uparrow} c^\dagger_{d\downarrow} c_{0\downarrow} c_{0\uparrow}$. It can be seen from the figure that while the spin-flip fluctuations decrease (since the Kondo cloud is formed out of these spin-flip fluctuations, this is consistent with the destruction of the Kondo cloud discussed in this paragraph), the pair fluctuations pick up. Since the spin subspace and charge subspace cannot coincide on the same site, we can then conclude that it is the growth of these pair fluctuations brought about by the presence of the purely local interaction U_b that make the screening of the impurity spin very poor.

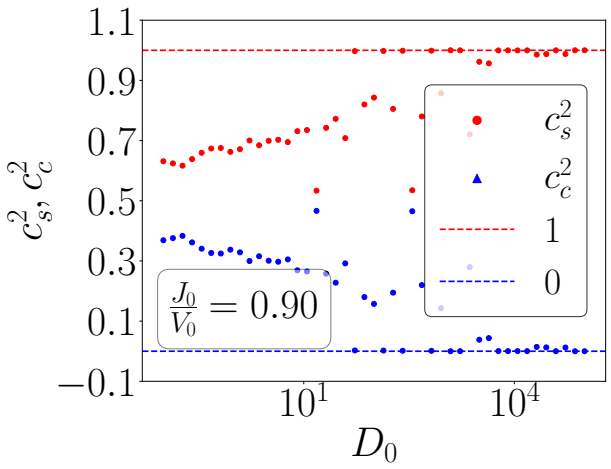

FIG. 8. Variation of spin and charge fractions, c_s and c_c, of the ground state, as a function of bare bandwidth D_0. Left and right panels show the cases of $J_0 < V_0$ and $J_0 > V_0$ respectively.

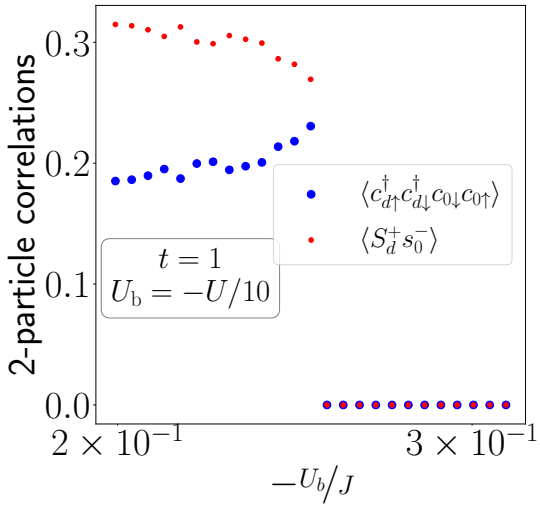

FIG. 9. Growth of pair fluctuations $p_d^\dagger p_0$ between the impurity and the zeroth site towards the critical point, $p^\dagger = c_\uparrow^\dagger c_\downarrow^\dagger$ being the local pair creation operator. This comes at the cost of the spin-flip fluctuations $S_d^+ s_0^-$ + h.c.. which decrease towards the transition.

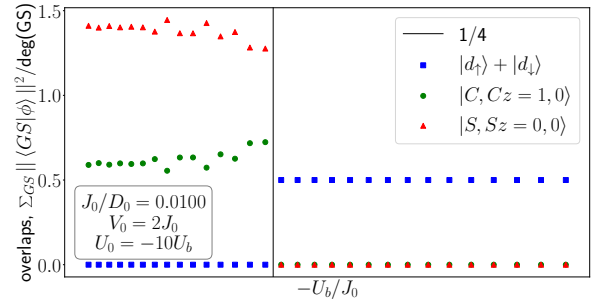

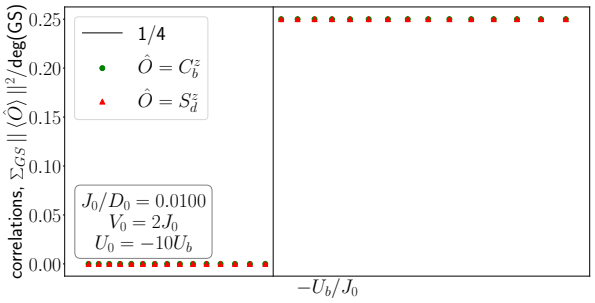

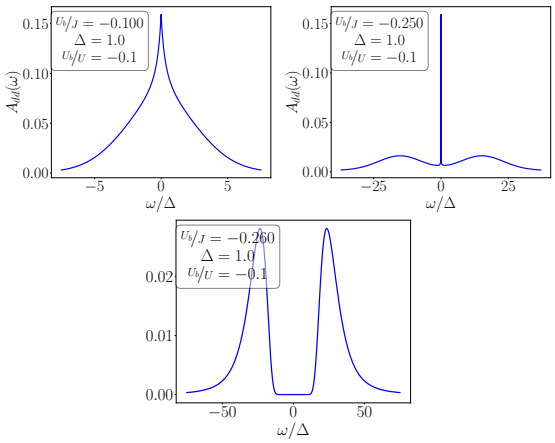

VII. CONCLUSIONS

- discuss why the model is minimal

Correlations in ground state

B. Impurity spectral function $A_{dd}(\omega)$

These are the frequency-domain spectral functions for the retarded propagator $-i\theta(t)\left\langle\left\{c_{d\sigma}(t), c_{d\sigma}^\dagger\right\}\right\rangle$:

ACKNOWLEDGMENTS

Abhirup Mukherjee thanks IISER Kolkata for funding through a research fellowship. S. Lal thanks the SERB, Govt. of India for funding through MATRICS grant MTR/2021/000141 and Core Research Grant CRG/2021/000852.

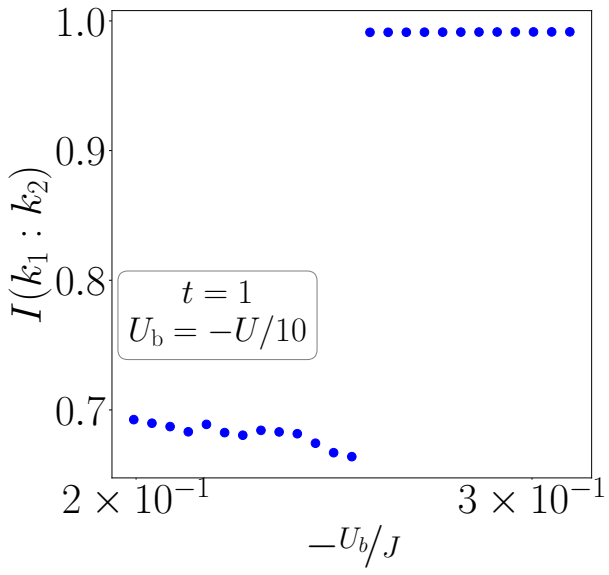
1.0
0.9
0.8
0.7
$I(k_1 : k_2)$
$t = 1$
$U_\mathrm{b} = -U/10$
2×10^{-1}
3×10^{-1}
$-U_b/J$

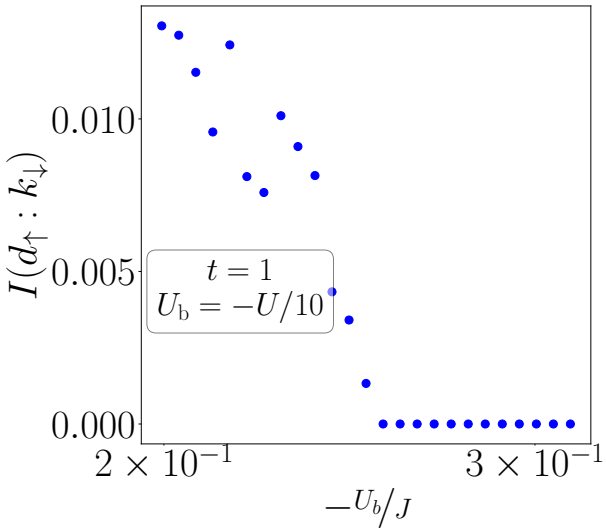
0.010
0.005
0.000
$I(d_\uparrow : k_\downarrow)$
$t = 1$
$U_\mathrm{b} = -U/10$
2×10^{-1}
3×10^{-1}
$-U_b/J$

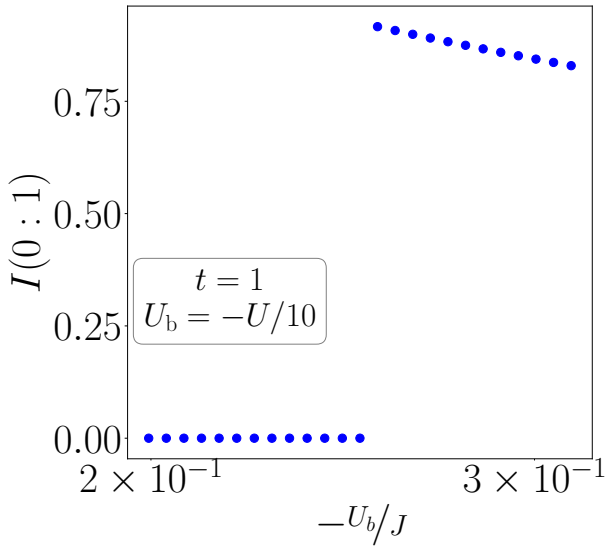
0.75
0.50
0.25
0.00
$I(0 : 1)$
$t = 1$
$U_\mathrm{b} = -U/10$
2×10^{-1}
3×10^{-1}
$-U_b/J$

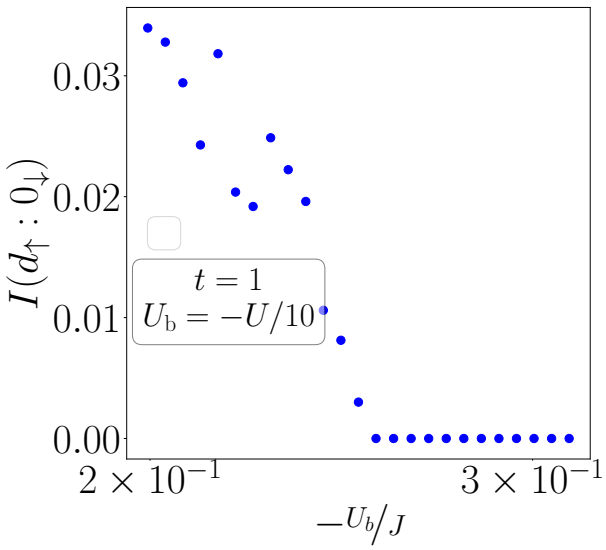
0.03
0.02
0.01
0.00
$I(d_\uparrow : 0_\downarrow)$
$t = 1$
$U_\mathrm{b} = -U/10$
2×10^{-1}
3×10^{-1}
$-U_b/J$

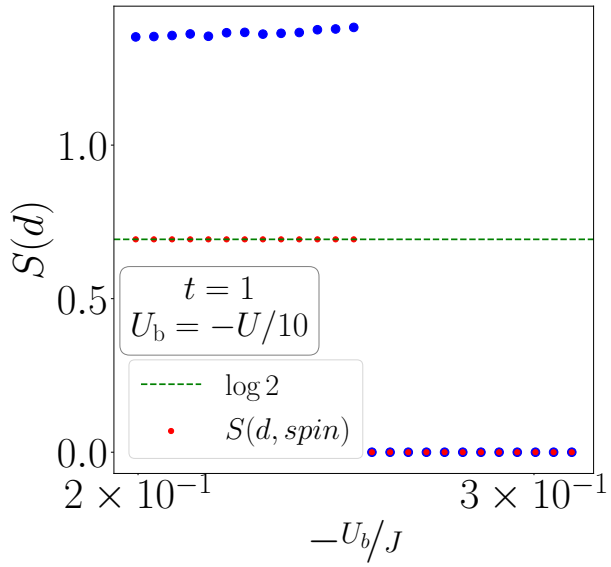
1.0
0.5
0.0
$S(d)$
$t = 1$
$U_\mathrm{b} = -U/10$
$\log 2$
$S(d, spin)$
2×10^{-1}
3×10^{-1}
$-U_b/J$

Appendix: Derivation of RG equations for the generalised Anderson impurity model

1. Renormalisation of the impurity energy ϵ_d

The coupling ϵ_d is renormalised by three kinds of vertices: V^2, J^2 and K^2. We will consider these processes one after another. We define n_j as the number of states being decoupled on each side of the Fermi surface, at the j^{th} RG step. In order to treat both spin and isospin exchanges democratically, we take $|\Psi\rangle_i = \frac{1}{2}\left(|0\rangle + |q\uparrow\rangle + |q\downarrow\rangle + |q\uparrow, q\downarrow\rangle\right)$ as the *initial* state for the scattering processes. The intermediate states $|\Psi\rangle_{\text{int}}$ in the particle sector ($c_{q\beta}|\Psi\rangle_i$) and hole sector $\left(c^\dagger_{q\beta}|\Psi\rangle_i\right)$ will then have both spin and isospin excitations which can couple with the corresponding impurity degree of freedom. We will assume that states $q > k_F$ ($\epsilon_q > 0$) above the Fermi surface can have only particle excitations and states below the Fermi surface can only have hole excitations. The kinetic energy part $\epsilon_q \tau_{q\beta}$ of H_D for $|\Psi\rangle_i$ is then zero, whereas it is always $D/2$ for $|\Psi\rangle_{\text{int}}$. To demonstrate this for a typical $q < k_F$, the hole excitation is $c_{q\uparrow}|\Psi\rangle_i = \frac{1}{\sqrt{2}}\left(|0\rangle + |q\downarrow\rangle\right)$. This has an isospin term in the form of the *holon* and a spin term in the form of the down state. Since $\tau_{q\uparrow} = -\frac{1}{2}$ in the excited state, the kinetic energy for $|\Psi\rangle_{\text{int}}$ is $\epsilon_q\tau_{q\uparrow} = (-D)\times\left(-\frac{1}{2}\right) = D/2$.

The renormalisation arising from the first kind of terms, in the particle sector, is

$$\sum_{q\beta} c^\dagger_{q\beta} c_{d\beta} \frac{V^2}{\omega - H_D} c^\dagger_{d\beta} c_{q\beta} = \sum_{q\beta} V^2 \hat{n}_{q\beta}\left(1-\hat{n}_{d\beta}\right)\left(\frac{1-\hat{n}_{d\overline{\beta}}}{\omega - E_0} + \frac{\hat{n}_{d\overline{\beta}}}{\omega' - E_1}\right) = V^2 n_j \sum_{\beta}\left(1-\hat{n}_{d\beta}\right)\left(\frac{1-\hat{n}_{d\overline{\beta}}}{\omega_0 - E_0} + \frac{\hat{n}_{d\overline{\beta}}}{\omega_1 - E_1}\right) \tag{A.1}$$

q runs over the momentum states that are being decoupled at this RG step: $|q| = \Lambda_j$. $E_{1,0}$ are the diagonal parts of the Hamiltonian at $\hat{n}_{d\overline{\beta}} = 1, 0$ respectively. We have $\hat{n}_{d\beta} = 1$ in the intermediate state because of the $c^\dagger_{d\beta}$ in front of the Greens function. Applying $c_{q\beta}$ on the initial state $|\Psi\rangle_i$ leaves us with $C^z_q = -\frac{1}{2}$ and $s^z_q = \frac{1}{2}\overline{\beta}$. We also know that

$$\hat{n}_{d\beta} = 1, \begin{cases} \hat{n}_{d\overline{\beta}} = 0 & \implies S^z_d = \frac{1}{2}\beta, C^z_d = 0, \epsilon_d\left(\hat{n}_{d\uparrow} - \hat{n}_{d\downarrow}\right)^2 = \epsilon_d \\ \hat{n}_{d\overline{\beta}} = 1 & \implies S^z_d = 0, C^z_d = \frac{1}{2}, \epsilon_d\left(\hat{n}_{d\uparrow} - \hat{n}_{d\downarrow}\right)^2 = 0 \end{cases} \tag{A.2}$$

Combining all this, we can write $E_1 = \frac{D}{2} - \frac{K}{4}$ and $E_0 = \frac{D}{2} + \epsilon_d - \frac{J}{4}$. In order to relate ω_0 with ω_1 with the common fluctuation scale ω for the conduction electrons, we will replace these quantum fluctuation scales by the current renormalised values of the single-particle self-energy for the initial state from which we started scattering. For $\hat{n}_{d\overline{\beta}} = 0$, there is no additional self-energy because the impurity does not have any spin: $\omega_0 = \omega$. For $\hat{n}_{d\overline{\beta}} = 1$, we have an additional self-energy of ϵ_d arising from the correlation on the impurity: $\omega_1 = \omega + \epsilon_d$. Substituting the values of $E_{0,1}$ and $\omega_{0,1}$, we get

$$V^2 n_j \sum_{\beta}\left(1-\hat{n}_{d\beta}\right)\left(\frac{1-\hat{n}_{d\overline{\beta}}}{\omega - \frac{D}{2} - \epsilon_d + \frac{J}{4}} + \frac{\hat{n}_{d\overline{\beta}}}{\omega - \frac{D}{2} + \epsilon_d + \frac{K}{4}}\right) \tag{A.3}$$

Performing a similar calculation for the hole sector gives the contribution:

$$V^2 n_j \sum_{\beta}\hat{n}_{d\beta}\left(\frac{1-\hat{n}_{d\overline{\beta}}}{\omega - \frac{D}{2} + \epsilon_d + \frac{K}{4}} + \frac{\hat{n}_{d\overline{\beta}}}{\omega - \frac{D}{2} - \epsilon_d + \frac{J}{4}}\right) \tag{A.4}$$

We now come to the second type of terms: spin-spin. We first look at the particle sector:

$$\frac{J^2}{4}\sum_{q\beta} c^\dagger_{d\overline{\beta}} c_{d\beta} c^\dagger_{q\beta} c_{-q\overline{\beta}} \frac{1}{\omega - H_D} c^\dagger_{d\beta} c_{d\overline{\beta}} c^\dagger_{q\overline{\beta}} c_{q\beta} = \frac{J^2}{4} n_j \frac{1}{\omega - \frac{D}{2} + \frac{J}{4}} \sum_{\beta}\hat{n}_{d\overline{\beta}}\left(1-\hat{n}_{d\beta}\right) \tag{A.5}$$

The diagonal part in the denominator was simple to deduce in this case, because the nature of the scattering requires the spins S^z_d and $\frac{\beta}{2}\left(\hat{n}_{q\beta} - \hat{n}_{q\overline{\beta}}\right)$ to be anti-parallel. This ensures that the intermediate state has an energy of $E = \frac{D}{2} + \epsilon_d - \frac{J}{4}$, and the quantum fluctuation scale is $\omega' = \omega + \epsilon_d$, such that $\omega' - E = \omega - \frac{D}{2} + \frac{J}{4}$. In the hole sector, we have

$$\frac{J^2}{4} n_j \frac{1}{\omega - \frac{D}{2} + \frac{J}{4}} \sum_{\beta}\hat{n}_{d\beta}\left(1-\hat{n}_{d\overline{\beta}}\right) \tag{A.6}$$

The final kind of scattering is the K^2 type. Similar to the J^2 term, we get the following contribution:

$$\frac{K^2}{4}\sum_{q\beta} c^\dagger_{q\beta}c^\dagger_{q\overline{\beta}}c_{d\overline{\beta}}c_{d\beta}\frac{1}{\omega - H_D}c^\dagger_{d\beta}c^\dagger_{d\overline{\beta}}c_{q\overline{\beta}}c_{q\beta} = \frac{K^2}{2}n_j\frac{1}{\omega - \frac{D}{2} + \frac{K}{4}}\left(1-\hat{n}_{d\uparrow}\right)\left(1-\hat{n}_{d\downarrow}\right) \tag{A.7}$$

in the particle sector. This is again because $E = \frac{D}{2} - \frac{K}{4}$ in the intermediate state and $\omega' = \omega$. In the hole sector, we get

$$\frac{K^2}{2}n_j\frac{1}{\omega - \frac{D}{2} + \frac{K}{4}}\hat{n}_{d\uparrow}\hat{n}_{d\downarrow}\ . \tag{A.8}$$

We now have all possible renormalisation to the impurity energy ϵ_d. To actually compute the renormalisation, we will first calculate the renormalisation in the energies ϵ_0, ϵ_1 and ϵ_2 of the impurity states $|\hat{n}_d = 0\rangle, |\hat{n}_d = 1\rangle, |\hat{n}_d = 2\rangle$ respectively. The renormalisation of these states are given by the following terms:

- $\Delta\epsilon_0$ is given by the renormalisation of the term $\left(1-\hat{n}_{d\uparrow}\right)\left(1-\hat{n}_{d\downarrow}\right)$
- $\Delta\epsilon_1$ is given by the renormalisation of either $\left(1-\hat{n}_{d\uparrow}\right)\hat{n}_{d\downarrow}$ or $\left(1-\hat{n}_{d\downarrow}\right)\hat{n}_{d\uparrow}$
- $\Delta\epsilon_2$ is given by the renormalisation of $\hat{n}_{d\uparrow}\hat{n}_{d\downarrow}$

From eqs. A.3, A.4, A.5, A.6, A.7 and A.8, we write

$$\Delta\epsilon_0 = \Delta\epsilon_2 = \frac{2V^2n_j}{\omega - \frac{D}{2} - \epsilon_d + \frac{J}{4}} + \frac{K^2n_j/2}{\omega - \frac{D}{2} + \frac{K}{4}}, \quad \Delta\epsilon_1 = \frac{2V^2n_j}{\omega - \frac{D}{2} + \epsilon_d + \frac{K}{4}} + \frac{J^2n_j/2}{\omega - \frac{D}{2} + \frac{J}{4}} \tag{A.9}$$

We had started with a particle-hole symmetric Hamiltonian ($2\epsilon_d + U = 0$); the fact that $\Delta\epsilon_0 = \Delta\epsilon_2$ means the RG transformation has preserved that symmetry. The renormalisation of ϵ_d is simply the renormalisation in the energy difference between the singly-occupied and vacant impurity levels: $\Delta\epsilon_d = \Delta\epsilon_1 - \Delta\epsilon_0$. This gives our first RG equation:

$$\Delta\epsilon_d = 2V^2n_j\left(\frac{1}{\omega - \frac{D}{2} + \epsilon_d + \frac{K}{4}} - \frac{1}{\omega - \frac{D}{2} - \epsilon_d + \frac{J}{4}}\right) + \frac{n_j}{2}\left(\frac{J^2}{\omega - \frac{D}{2} + \frac{J}{4}} - \frac{K^2}{\omega - \frac{D}{2} + \frac{K}{4}}\right) \tag{A.10}$$

2. Renormalisation of the hybridisation V

Renormalisation of V happens through two kinds of processes: VJ and VK. In order words, the two vertices involve one single-particle scattering and one spin or isospin exchange respectively. We first look at the vertices that involve a spin-exchange scattering.

Within spin-exchange, the scattering can be either via S^z_d or through $S^\pm_d$. For the first kind, we have the following contribution in the particle sector:

$$\sum_{q\beta} Vc^\dagger_{q\beta}c_{d\beta}\frac{1}{\omega - H_D}\frac{1}{4}J\sum_k\left(\hat{n}_{d\beta} - \hat{n}_{d\overline{\beta}}\right)c^\dagger_{k\beta}c_{q\beta} = \frac{1}{4}VJn_j\frac{1}{2}\left(\frac{1}{\omega'_1 - E} + \frac{1}{\omega'_2 - E}\right)\sum_{k\beta}\left(1-\hat{n}_{d\overline{\beta}}\right)c_{d\beta}c^\dagger_{k\beta} \tag{A.11}$$

The transformation from $\frac{1}{\omega - H_D}$ to $\frac{1}{2}\left(\frac{1}{\omega'_1 - E} + \frac{1}{\omega'_2 - E}\right)$ is made so that we can account for both the initial state and the final state energies through the two fluctuation scales ω'_1 and ω'_2 respectively; we calculate the denominators for both the initial and final states, and then take the mean of the two (hence the factor of half in front). This was not required previously because in the earlier scattering processes, the impurity returned to its initial state at the end, at least in terms of $\epsilon_d\left(\hat{n}_{d\uparrow} - \hat{n}_{d\downarrow}\right)^2$, and so we had $\omega'_1 = \omega'_2 = \omega'$.

Note that the $c_{d\beta}$ in front of the Greens function resulted in $\left(\hat{n}_{d\beta} - \hat{n}_{d\overline{\beta}}\right) \to \left(1 - \hat{n}_{d\overline{\beta}}\right)$. The intermediate state is characterised by $\hat{n}_{d\beta} = 1 - \hat{n}_{d\overline{\beta}} = 1$, which means that $E = \frac{D}{2} + \epsilon_d - \frac{J}{4}$. Moreover, the initial state gives $\omega'_1 = \omega + \epsilon_d$ while the final state gives $\omega'_2 = \omega$. Therefore, the renormalisation becomes

$$-\frac{n_j}{4}VJ\frac{1}{2}\left(\frac{1}{\omega - \frac{D}{2} + \frac{J}{4}} + \frac{1}{\omega - \frac{D}{2} - \epsilon_d + \frac{J}{4}}\right)\sum_{k\beta}\left(1-\hat{n}_{d\overline{\beta}}\right)c^\dagger_{k\beta}c_{d\beta} \tag{A.12}$$

One can generate another such process by exchanging the single-particle process and the spin-exchange process:

$$\sum_{q\beta}\frac{1}{4}J\sum_{k}\left(\hat{n}_{d\beta}-\hat{n}_{d\overline{\beta}}\right)c^{\dagger}_{q\beta}c_{k\beta}\frac{1}{\omega-H_D}Vc^{\dagger}_{d\beta}c_{q\beta} \tag{A.13}$$

This is simply the Hermitian conjugate of the previous contribution. Combining this with the previous then gives

$$-\frac{n_j}{8}VJ\left(\frac{1}{\omega-\frac{D}{2}+\frac{J}{4}}+\frac{1}{\omega-\frac{D}{2}-\epsilon_d+\frac{J}{4}}\right)\sum_{k\beta}\left(1-\hat{n}_{d\overline{\beta}}\right)\left(c^{\dagger}_{d\beta}c_{k\beta}+\text{h.c.}\right) \tag{A.14}$$

We now consider the spin-exchange processes involving $S^{\pm}_d$:

$$\sum_{q\beta}Vc^{\dagger}_{q\beta}c_{d\beta}\frac{1}{\omega-H_D}\frac{1}{2}J\sum_{k}c^{\dagger}_{d\beta}c_{d\overline{\beta}}c^{\dagger}_{k\overline{\beta}}c_{q\beta}=\frac{1}{2}VJn_j\frac{1}{2}\left(\frac{1}{\omega'_1-E}+\frac{1}{\omega'_2-E}\right)\sum_{k\beta}\left(1-\hat{n}_{d\beta}\right)c_{d\overline{\beta}}c^{\dagger}_{k\overline{\beta}} \tag{A.15}$$

We again have $E=\frac{D}{2}+\epsilon_d-\frac{J}{4},\omega'_1=\omega+\epsilon_d$ and $\omega'_2=\omega$, which gives

$$-\frac{1}{4}VJn_j\left(\frac{1}{\omega-\frac{D}{2}+\frac{J}{4}}+\frac{1}{\omega-\frac{D}{2}-\epsilon_d+\frac{J}{4}}\right)\sum_{k\beta}\left(1-\hat{n}_{d\beta}\right)c^{\dagger}_{k\overline{\beta}}c_{d\overline{\beta}} \tag{A.16}$$

Combining this with the Hermitian conjugate obtained from exchanging the processes gives

$$-\frac{1}{4}VJn_j\left(\frac{1}{\omega-\frac{D}{2}+\frac{J}{4}}+\frac{1}{\omega-\frac{D}{2}-\epsilon_d+\frac{J}{4}}\right)\sum_{k\beta}\left(1-\hat{n}_{d\beta}\right)\left(c^{\dagger}_{k\overline{\beta}}c_{d\overline{\beta}}+\text{h.c.}\right) \tag{A.17}$$

The contributions from the hole sector are obtained making the transformation $\hat{n}_{d\overline{\beta}}\to 1-\hat{n}_{d\overline{\beta}}$ on the particle sector contributions. The total renormalisation to V from VJ processes are

$$-\frac{3n_j}{8}VJ\left(\frac{1}{\omega-\frac{D}{2}+\frac{J}{4}}+\frac{1}{\omega-\frac{D}{2}-\epsilon_d+\frac{J}{4}}\right)\sum_{k\beta}\left(c^{\dagger}_{d\beta}c_{k\beta}+\text{h.c.}\right) \tag{A.18}$$

We now look at the VK processes. The first one is

$$\sum_{q\beta}Vc^{\dagger}_{q\beta}c_{d\beta}\frac{1}{\omega-H_D}\frac{1}{4}K\sum_{k}\left(\hat{n}_d-1\right)c^{\dagger}_{k\beta}c_{q\beta}=-\frac{1}{8}VKn_j\left(\frac{1}{\omega-\frac{D}{2}+\frac{K}{4}}+\frac{1}{\omega-\frac{D}{2}+\epsilon_d+\frac{K}{4}}\right)\sum_{k\beta}\hat{n}_{d\overline{\beta}}c^{\dagger}_{k\beta}c_{d\beta} \tag{A.19}$$

The exchanged process again gives the Hermitian conjugate, so the combined contribution is

$$-\frac{1}{8}VKn_j\left(\frac{1}{\omega-\frac{D}{2}+\frac{K}{4}}+\frac{1}{\omega-\frac{D}{2}+\epsilon_d+\frac{K}{4}}\right)\sum_{k\beta}\hat{n}_{d\overline{\beta}}\left(c^{\dagger}_{k\beta}c_{d\beta}+\text{h.c.}\right) \tag{A.20}$$

The isospin-flip vertex gives

$$\sum_{q\beta}Vc^{\dagger}_{q\beta}c_{d\beta}\frac{1}{\omega-H_D}\frac{1}{2}K\sum_{k}c^{\dagger}_{d\beta}c^{\dagger}_{d\overline{\beta}}c_{k\overline{\beta}}c_{q\beta}=\frac{1}{4}KVn_j\left(\frac{1}{\omega-\frac{D}{2}+\frac{K}{4}}+\frac{1}{\omega-\frac{D}{2}+\epsilon_d+\frac{K}{4}}\right)\sum_{k\beta}\left(1-\hat{n}_{d\beta}\right)c^{\dagger}_{d\overline{\beta}}c_{k\overline{\beta}}\ . \tag{A.21}$$

Combining with Hermitian conjugate gives

$$\frac{1}{4}KVn_j\left(\frac{1}{\omega-\frac{D}{2}+\frac{K}{4}}+\frac{1}{\omega-\frac{D}{2}+\epsilon_d+\frac{K}{4}}\right)\sum_{k\beta}\left(1-\hat{n}_{d\beta}\right)\left(c^{\dagger}_{d\overline{\beta}}c_{k\overline{\beta}}+\text{h.c.}\right)\ . \tag{A.22}$$

After obtaining the hole sector contributions, the total renormalisation from VK processes is

$$-\frac{3n_j}{4}VK\left(\frac{1}{\omega-\frac{D}{2}+\frac{K}{4}}+\frac{1}{\omega-\frac{D}{2}+\epsilon_d+\frac{K}{4}}\right)\sum_{k\beta}\left(c^{\dagger}_{d\beta}c_{k\beta}+\text{h.c.}\right)\ . \tag{A.23}$$

The RG equation for V is

$$\Delta V=-\frac{3n_jV}{8}\left[J\left(\frac{1}{\omega-\frac{D}{2}+\frac{J}{4}}+\frac{1}{\omega-\frac{D}{2}-\epsilon_d+\frac{J}{4}}\right)+K\left(\frac{1}{\omega-\frac{D}{2}+\frac{K}{4}}+\frac{1}{\omega-\frac{D}{2}+\epsilon_d+\frac{K}{4}}\right)\right] \tag{A.24}$$

3. Renormalisation of the exchange couplings J and K

We will just note the renormalisation in J^z, which will be equal to $J^{\pm}$ due to spin-rotation symmetry. The terms that renormalise J^z are of the form $S_d^{\pm}S_d^{\mp}$. In the particle sector, we have

$$\sum_q \sum_{kk'} \frac{1}{4} J^2 S_d^{\pm} c_{q\mp}^{\dagger} c_{k'\pm} \frac{1}{\omega - H_D} S_d^{\mp} c_{k\pm}^{\dagger} c_{q\mp} = -n_j \frac{1}{4} J^2 \left(\frac{1}{2} \pm S_d^z\right) \sum_{kk'} c_{k\pm}^{\dagger} c_{k\pm} \frac{1}{\omega - \frac{D}{2} + \frac{J}{4}} \cdot \tag{A.25}$$

The denominator is determined using $E = \frac{D}{2} + \epsilon_d - \frac{J}{4}$ and $\omega' = \omega + \epsilon_d$. In the hole sector, we similarly have

$$\sum_q \sum_{kk'} \frac{1}{4} J^2 S_d^{\mp} c_{k\pm}^{\dagger} c_{q\mp} \frac{1}{\omega - H_D} S_d^{\pm} c_{q\mp}^{\dagger} c_{k'\pm} = n_j \frac{1}{4} J^2 \left(\frac{1}{2} \mp S_d^z\right) \sum_{kk'} c_{k\pm}^{\dagger} c_{k\pm} \frac{1}{\omega - \frac{D}{2} + \frac{J}{4}} \cdot \tag{A.26}$$

Adding all four expressions and dropping the constant part, we get

$$-n_j \frac{1}{2} J^2 S_d^z \sum_{kk'} \left(c_{k\uparrow}^{\dagger} c_{k'\uparrow} - c_{k\downarrow}^{\dagger} c_{k'\downarrow}\right) \frac{1}{\omega - \frac{D}{2} + \frac{J}{4}} \cdot \tag{A.27}$$

We can now directly read off the RG equation for J:

$$\Delta J = -\frac{n_j J^2}{\omega - \frac{D}{2} + \frac{J}{4}} \tag{A.28}$$

Since the spin and charge degrees of freedom are treated on an equal footing in the model, we obtain the RG equation for K by simply changing $J \to K$:

$$\Delta K = -\frac{n_j K^2}{\omega - \frac{D}{2} + \frac{K}{4}} \tag{A.29}$$

Appendix: U_b-included terms

We first Fourier transform the U_b-term to $k-$space. In $k-$space, the diagonal contribution (to H_D) coming from this term is the single-particle self-energy $-U_b \left(\hat{n}_{q\beta}\right)^2$ which can be made particle-hole symmetric in the form:

$$-U_b \left(\tau_{q\beta}\right)^2 \tag{A.1}$$

where q is the $k-$state being decoupled and $\tau \equiv \hat{n} - 1/2$. In the initial state $|\Psi\rangle_i$, we have $\langle \hat{n}_{q\beta} \rangle = 1/2 \implies \tau_{q\beta} = 0$, so the contribution of U_b to that state is 0. For both hole excitations $c_{q\beta} |\Psi\rangle_i$ as well as particle excitations $c_{q\beta}^{\dagger} |\Psi\rangle_i$, the intermediate state energy lowers to $-U_b/4$.

The off-diagonal part is

$$-\frac{U_b}{2} \sum_{kk'\sigma} c_{k\sigma}^{\dagger} c_{k'\sigma} + U_b \sum_{k_1,k_2,k_1',k_2'} c_{k_1\uparrow}^{\dagger} c_{k_2\uparrow} c_{k_1'\downarrow}^{\dagger} c_{k_2'\downarrow} \tag{A.2}$$

We ignore the potential scattering arising from the first term.

1. Renormalisation of U_b

U_b can renormalise only via itself. The relevant renormalisation term in the particle sector is

$$U_b^2 \sum_{q\beta} \sum_{k_1,k_2,k_3,k_1',k_2',k_3'} c_{q\beta}^{\dagger} c_{k_1\beta} c_{k_3\overline{\beta}}^{\dagger} c_{k_1'\overline{\beta}} \frac{1}{\omega - H_D} c_{k_2'\overline{\beta}}^{\dagger} c_{k_3'\overline{\beta}} c_{k_2\beta}^{\dagger} c_{q\beta} \tag{A.3}$$

In order to renormalise U_b, we need to contract one more pair of momenta. There are two choices. The first is by setting $k_3 = k_3' = q$. The two internal states, then, are $q\beta$ and $q\overline{\beta}$. As discussed above, the intermediate state energy is $-U_b/4$. We therefore have

$$\frac{U_b^2 n_j}{\omega - D/2 + U_b/4} \sum_{\beta} \sum_{k_1,k_2,k_1',k_2'} c_{k_1\beta} c_{k_1'\overline{\beta}} c_{k_2'\overline{\beta}}^{\dagger} c_{k_2\beta}^{\dagger} = \frac{U_b^2 n_j}{\omega - D/2 + U_b/4} \sum_{\beta} \sum_{k_1,k_2,k_1',k_2'} c_{k_2'\overline{\beta}}^{\dagger} c_{k_1'\overline{\beta}} c_{k_2\beta}^{\dagger} c_{k_1\beta} \tag{A.4}$$

Another way to contract the momenta is by setting $k_1' = k_2' = q$, which gives a renormalisation of

$$\frac{U_b^2 n_j}{\omega - D/2 + U_b/4} \sum_\beta \sum_{k_1,k_2,k_3,k_3'} c_{k_1\beta} c^\dagger_{k_3\overline{\beta}} c_{k_3'\overline{\beta}} c^\dagger_{k_2\beta} = -\frac{U_b^2 n_j}{\omega - D/2} \sum_\beta \sum_{k_1,k_2,k_3,k_3'} c^\dagger_{k_3\overline{\beta}} c_{k_3'\overline{\beta}} c^\dagger_{k_2\beta} c_{k_1\beta} \tag{A.5}$$

The two contributions cancel each other. The same cancellation happens in the hole sector as well.

2. Renormalisation of U

U_b does not have any new renormalisation term on account of U_b. U_b does however modify the existing RG equation for U, by shifting the denominator. The existing RG equation is

$$\Delta U = -4V^2 n_j \left(\frac{1}{\omega - \frac{D}{2} + \epsilon_d + \frac{K}{4}} - \frac{1}{\omega - \frac{D}{2} - \epsilon_d + \frac{J}{4}} \right) - n_j \left(\frac{J^2}{\omega - \frac{D}{2} + \frac{J}{4}} - \frac{K^2}{\omega - \frac{D}{2} + \frac{K}{4}} \right) . \tag{A.6}$$

On accounting for the contribution of U_b to the denominator, we get

$$\Delta U = -4V^2 n_j \left(\frac{1}{\omega - \frac{D}{2} + \frac{U_b}{4} + \epsilon_d + \frac{K}{4}} - \frac{1}{\omega - \frac{D}{2} + \frac{U_b}{4} - \epsilon_d + \frac{J}{4}} \right) - n_j \left(\frac{J^2}{\omega - \frac{D}{2} + \frac{U_b}{4} + \frac{J}{4}} - \frac{K^2}{\omega - \frac{D}{2} + \frac{U_b}{4} + \frac{K}{4}} \right) . \tag{A.7}$$

3. Renormalisation of V

The single-particle hybridisation V renormalises through terms of VU_b and U_bV kind. The first term gives

$$\begin{aligned} &\sum_{q\beta} \sum_k U_b V c^\dagger_{q\beta} c_{k\beta} \hat{n}_{q\overline{\beta}} \frac{1}{\omega - H_D} c^\dagger_{d\beta} c_{q\beta} \\ &= n_j U_b V \sum_{k\beta} c_{k\beta} \left[\frac{\hat{n}_{d\overline{\beta}}}{2} \left(\frac{1}{\omega_1 - E_1} + \frac{1}{\omega_1' - E_1} \right) + \frac{1 - \hat{n}_{d\overline{\beta}}}{2} \left(\frac{1}{\omega_0 - E_0} + \frac{1}{\omega_0' - E_0} \right) \right] c^\dagger_{d\beta} \end{aligned} \tag{A.8}$$

E_1 and E_0 are the intermediate state energies for $\hat{n}_{d\overline{\beta}} = 1$ and 0 respectively. $\omega_{1,0}$ are the quantum fluctuation scales for the corresponding initial states. $\omega'_{1,0}$ are the fluctuation scales for the corresponding final states. The intermediate energies are $E_1 = D/2 - U_b/4 - K/4, \quad E_0 = D/2 - U_b/4 - U/2 - J/4$. The fluctuation scales are $\omega_1 = \omega - U/2 = \omega_0', \quad \omega_1' = \omega = \omega_0$. Substituting these gives

$$\begin{aligned} -n_j U_b V \sum_{k\beta} c^\dagger_{d\beta} c_{k\beta} \Bigg[&\frac{\hat{n}_{d\overline{\beta}}}{2} \left(\frac{1}{\omega - \frac{D}{2} - \frac{U}{2} + \frac{U_b}{4} + \frac{K}{4}} + \frac{1}{\omega - \frac{D}{2} + \frac{U_b}{4} + \frac{K}{4}} \right) \\ &+ \frac{1 - \hat{n}_{d\overline{\beta}}}{2} \left(\frac{1}{\omega - \frac{D}{2} + \frac{U_b}{4} + \frac{U}{2} + \frac{J}{4}} + \frac{1}{\omega - \frac{D}{2} + \frac{U_b}{4} + \frac{J}{4}} \right) \Bigg] \end{aligned} \tag{A.9}$$

The second term is of the form

$$\sum_{q\beta} \sum_k U_b V c^\dagger_{q\beta} c_{d\beta} \frac{1}{\omega - H_D} \hat{n}_{q\overline{\beta}} c^\dagger_{k\beta} c_{q\beta} \tag{A.10}$$

and this is just the Hermitian conjugate of the previous term, so these two terms together lead to

$$\begin{aligned} -n_j U_b V \sum_{k\beta} \left(c^\dagger_{d\beta} c_{k\beta} + \text{h.c.} \right) \Bigg[&\frac{\hat{n}_{d\overline{\beta}}}{2} \left(\frac{1}{\omega - \frac{D}{2} - \frac{U}{2} + \frac{U_b}{4} + \frac{K}{4}} + \frac{1}{\omega - \frac{D}{2} + \frac{U_b}{4} + \frac{K}{4}} \right) \\ &+ \frac{1 - \hat{n}_{d\overline{\beta}}}{2} \left(\frac{1}{\omega - \frac{D}{2} + \frac{U_b}{4} + \frac{U}{2} + \frac{J}{4}} + \frac{1}{\omega - \frac{D}{2} + \frac{U_b}{4} + \frac{J}{4}} \right) \Bigg] \end{aligned} \tag{A.11}$$

In the hole sector, we have

$$\begin{aligned}
&\sum_{q\beta}\sum_{k} U_b V \hat{n}_{q\bar{\beta}} c^\dagger_{k\beta} c_{q\beta} \frac{1}{\omega - H_D} c^\dagger_{q\beta} c_{d\beta} \\
&- \sum_{q\beta}\sum_{k} U_b V \left(1 - \hat{n}_{q\bar{\beta}}\right) c^\dagger_{k\beta} c_{q\beta} \frac{1}{\omega - H_D} c^\dagger_{q\beta} c_{d\beta} \\
&= -n_j U_b V \sum_{k\beta} c^\dagger_{k\beta} \left[\frac{\hat{n}_{d\bar{\beta}}}{2} \left(\frac{1}{\omega_1 - E_1} + \frac{1}{\omega_1' - E_1} \right) + \frac{1 - \hat{n}_{d\bar{\beta}}}{2} \left(\frac{1}{\omega_0 - E_0} + \frac{1}{\omega_0' - E_0} \right) \right] c_{d\beta}
\end{aligned} \tag{A.12}$$

$E_1 = D/2 - U_b/4 - U/2 - J/4$, $E_0 = D/2 - U_b/4 - K/4$. The fluctuation scales are $\omega_1 = \omega = \omega_0'$, $\omega_1' = \omega - U/2 = \omega_0$. Substituting these gives

$$\begin{aligned}
-n_j U_b V \sum_{k\beta} c^\dagger_{d\beta} c_{k\beta} \Bigg[&\frac{1 - \hat{n}_{d\bar{\beta}}}{2} \left(\frac{1}{\omega - \frac{D}{2} - \frac{U}{2} + \frac{U_b}{4} + \frac{K}{4}} + \frac{1}{\omega - \frac{D}{2} + \frac{U_b}{4} + \frac{K}{4}} \right) \\
&+ \frac{\hat{n}_{d\bar{\beta}}}{2} \left(\frac{1}{\omega - \frac{D}{2} + \frac{U_b}{4} + \frac{U}{2} + \frac{J}{4}} + \frac{1}{\omega - \frac{D}{2} + \frac{U_b}{4} + \frac{J}{4}} \right) \Bigg]
\end{aligned} \tag{A.13}$$

The other term, obtained by exchanging V and U_b, gives the Hermitian conjugate, so the overall contribution from the hole sector is the same as the total contribution from the particle sector, but with $\hat{n}_{d\bar{\beta}} \to 1 - \hat{n}_{d\bar{\beta}}$. Combining both the sectors, we get

$$\begin{aligned}
-n_j U_b V \sum_{k\beta} \left(c^\dagger_{d\beta} c_{k\beta} + \text{h.c.} \right) \frac{1}{2} \Bigg[&\left(\frac{1}{\omega - \frac{D}{2} - \frac{U}{2} + \frac{U_b}{4} + \frac{K}{4}} + \frac{1}{\omega - \frac{D}{2} + \frac{U_b}{4} + \frac{K}{4}} \right) \\
&+ \left(\frac{1}{\omega - \frac{D}{2} + \frac{U_b}{4} + \frac{U}{2} + \frac{J}{4}} + \frac{1}{\omega - \frac{D}{2} + \frac{U_b}{4} + \frac{J}{4}} \right) \Bigg]
\end{aligned} \tag{A.14}$$

Combining with the already existing RG equations, the complete RG equation for V becomes

$$\begin{aligned}
\Delta V = &- \frac{3 n_j V}{8} \left[\left(\frac{J}{\omega - \frac{D}{2} + \frac{U_b}{4} + \frac{J}{4}} + \frac{J}{\omega - \frac{D}{2} + \frac{U_b}{4} + \frac{U}{2} + \frac{J}{4}} \right) + K \left(\frac{K}{\omega - \frac{D}{2} + \frac{U_b}{4} + \frac{K}{4}} + \frac{K}{\omega - \frac{D}{2} + \frac{U_b}{4} - \frac{U}{2} + \frac{K}{4}} \right) \right] \\
&- \frac{n_j U_b}{2} \left[\left(\frac{V}{\omega - \frac{D}{2} - \frac{U}{2} + \frac{U_b}{4} + \frac{K}{4}} + \frac{V}{\omega - \frac{D}{2} + \frac{U_b}{4} + \frac{K}{4}} \right) + \left(\frac{V}{\omega - \frac{D}{2} + \frac{U_b}{4} + \frac{U}{2} + \frac{J}{4}} + \frac{V}{\omega - \frac{D}{2} + \frac{U_b}{4} + \frac{J}{4}} \right) \right] \\
= &- \frac{n_j V}{8} \left[\left(\frac{3J + 4U_b}{\omega - \frac{D}{2} + \frac{U_b}{4} + \frac{J}{4}} + \frac{3J + 4U_b}{\omega - \frac{D}{2} + \frac{U_b}{4} + \frac{U}{2} + \frac{J}{4}} \right) + \left(\frac{3K + 4U_b}{\omega - \frac{D}{2} + \frac{U_b}{4} + \frac{K}{4}} + \frac{3K + 4U_b}{\omega - \frac{D}{2} + \frac{U_b}{4} - \frac{U}{2} + \frac{K}{4}} \right) \right]
\end{aligned} \tag{A.15}$$

4. Renormalisation of J and K

We will track the entire renormalisation purely from that of J^+, by virtue of the SU(2) symmetry. J^+ renormalises through the JU_b terms. One of the terms is

$$\frac{1}{2} J U_b \sum_{q} \sum_{k,k'} S^+_d c^\dagger_{q\downarrow} c_{k\uparrow} \frac{1}{\omega - H_D} \hat{n}_{q\uparrow} c^\dagger_{k'\downarrow} c_{q\downarrow} = -\frac{1}{2} \frac{J U_b n_j}{\omega - \frac{D}{2} + \frac{U_b}{2} + \frac{J}{4}} \sum_{k,k'} S^+_d c^\dagger_{k'\downarrow} c_{k\uparrow} \tag{A.16}$$

The factor of half in front is the same half factor that appears in front of the $S^+_1 S^-_2, S^-_1 S^+_2$ terms when we rewrite $\vec{S}_1 \cdot \vec{S}_2$ in terms of $S^z, S^\pm$. Another term is obtained by switching J and U_b:

$$\frac{1}{2} J U_b \sum_{q} \sum_{k,k'} \hat{n}_{q\downarrow} c^\dagger_{q\uparrow} c_{k\uparrow} \frac{1}{\omega - H_D} S^+_d c^\dagger_{k'\downarrow} c_{q\uparrow} = -\frac{1}{2} \frac{J U_b n_j}{\omega - \frac{D}{2} + \frac{U_b}{2} + \frac{J}{4}} \sum_{k,k'} S^+_d c^\dagger_{k'\downarrow} c_{k\uparrow} \tag{A.17}$$

The corresponding terms in the hole sector are

$$\frac{1}{2}JU_b\sum_q\sum_{k,k'}S_d^+c_{k'\downarrow}^\dagger c_{q\uparrow}\frac{1}{\omega-H_D}\hat{n}_{q\downarrow}c_{q\uparrow}^\dagger c_{k\uparrow}=-\frac{1}{2}\frac{JU_bn_j}{\omega-\frac{D}{2}+\frac{U_b}{2}+\frac{J}{4}}\sum_{k,k'}S_d^+c_{k'\downarrow}^\dagger c_{k\uparrow} \tag{A.18}$$

$$\frac{1}{2}JU_b\sum_q\sum_{k,k'}\hat{n}_{q\uparrow}c_{k'\downarrow}^\dagger c_{q\downarrow}\frac{1}{\omega-H_D}S_d^+c_{q\downarrow}^\dagger c_{k\uparrow}=-\frac{1}{2}\frac{JU_bn_j}{\omega-\frac{D}{2}+\frac{U_b}{2}+\frac{J}{4}}\sum_{k,k'}S_d^+c_{k'\downarrow}^\dagger c_{k\uparrow} \tag{A.19}$$

Adding all these terms and combining with the existing RG equation, we get the updated RG equation for J:

$$\Delta J=-Jn_j\frac{4U_b+J}{\omega-\frac{D}{2}+\frac{U_b}{2}+\frac{J}{4}} \tag{A.20}$$

[1] N. F. Mott, Proceedings of the Physical Society. Section A **62**, 416 (1949).
[2] K. Held, R. Peters, and A. Toschi, Phys. Rev. Lett. **110**, 246402 (2013).
[3] A. Mukherjee and S. Lal, New Journal of Physics **22**, 063007 (2020).
[4] A. Mukherjee and S. Lal, New Journal of Physics **22**, 063008 (2020).
[5] A. Mukherjee and S. Lal, Nuclear Physics B **960**, 115170 (2020).
[6] A. Mukherjee and S. Lal, Nuclear Physics B **960**, 115163 (2020).
[7] S. Patra and S. Lal, Phys. Rev. B **104**, 144514 (2021).
[8] S. Pal, A. Mukherjee, and S. Lal, New Journal of Physics **21**, 023019 (2019).
[9] A. Mukherjee, S. Patra, and S. Lal, Journal of High Energy Physics **04**, 148 (2021).
[10] A. Mukherjee and S. Lal, Journal of Physics: Condensed Matter **34**, 275601 (2022).
[11] A. Mukherjee, A. Mukherjee, N. S. Vidhyadhiraja, A. Taraphder, and S. Lal, Phys. Rev. B **105**, 085119 (2022).